Some Thermal Constraints on Crustal Assimilation during Fractionation of Hydrous, Mantle-derived Magmas with Examples from Central Alpine Batholiths

Author(s):
Thompson, Alan Bruce; Matile, Luzius; Ulmer, Peter

Publication date:
2002

Permanent link:
https://doi.org/10.3929/ethz-b-000422851

Originally published in:
Journal of Petrology 43(3), https://doi.org/10.1093/petrology/43.3.403

JOURNAL OF PETROLOGY | VOLUME 43 | NUMBER 3 | PAGES 403–422 | 2002

Some Thermal Constraints on Crustal Assimilation during Fractionation of Hydrous, Mantle-derived Magmas with Examples from Central Alpine Batholiths

ALAN BRUCE THOMPSON*, LUZIUS MATILE AND PETER ULMER

DEPARTMENT OF EARTH SCIENCES, ETH ZÜRICH, CH-8092, SWITZERLAND

RECEIVED MARCH 29, 1998; REVISED TYPESCRIPT ACCEPTED SEPTEMBER 1, 2001

We provide a model for the fractional crystallization of hydrous mantle-derived magma to form calc-alkaline plutons, based upon mass balance for geological examples of fractionation sequences in the lower continental crust. This is complemented by a thermal model for the heat budget obtained from a projected phase diagram and thermodynamic data. Fractional crystallization (FC) and assimilation–fractional crystallization (AFC) paths have been calculated with these models and the mass ratio of assimilation to crystallization as a function of parent magma type and temperature, crustal rock fertility and temperature, and mechanism of assimilation, have been determined. When these results are combined with F *(melt fraction) and* r *(ratio of mass assimilated/crystallized) values evaluated from geochemical data then new information, not available with the methods separately, can be deduced. This includes when and at what depth and temperature in the crust the assimilation took place, as well as the likely parent magma type and temperature of the assimilant. Our results are presented in simple graphical fashion to facilitate future studies that examine the evolution of individual calc-alkaline plutons and the mechanisms of crustal contamination, and to improve melt models involving hydrous magma in volcanic arcs and in the lower continental crust*

KEY WORDS: *assimilation; hydrous mantle magma; thermal models; fractional crystallization; magma mixing; Alpine batholiths; Adamello; Bergell*

INTRODUCTION

It is to be expected that high-temperature primitive mantle-derived magmas, during their passage through the crust, can melt and assimilate crustal rocks with low melting temperatures. Some magma chambers, particularly those beneath magmatic arcs, involve fractionation of hydrous, mantle-derived magmas generated in the 'mantle wedge' above subduction zones (e.g. Hildreth & Moorbath, 1988; Davies & Stevenson, 1992). However, mantle-derived magmas can also undergo closed-system fractional crystallization (FC) in crustal magma chambers, and to complicate matters the 'granitic' magmatic end products of FC processes are rather similar in general mineralogy and chemical composition to the 'granitic' partial melts of crustal rocks (e.g. Chappell & White, 1974). It is these latter melts that can be assimilated by a fractionating magma of mantle origin through an AFC process (i.e. assimilation during subsequent fractional crystallization). It is not yet well enough known just how the 'down-temperature' liquid line of descent, which determines the temperature–composition relations during fractional crystallization of high-temperature hydrous mantle-derived magmas, differs from the 'up-temperature' mixing trends of assimilation of partial melts from crustal rocks into mantle-derived magmas.

In the present study we use thermal constraints to evaluate the progress and efficiency of magma mixing following assimilation at different levels in the crust. We test by heat and mass balance the extent of assimilation of crustal 'country' rocks in different local 'plutonic' settings (e.g. stoped xenoliths, crust adjacent to sills) at various stages in an AFC process. We also examine how assimilation of crustal rocks affects the crystallization

*Corresponding author. Telephone: 41-1-632-3788. Fax: 41-1-632-1088. E-mail: alan.thompson@erdw.ethz.ch

interval of hydrous mantle-derived magmas, the fractionates of which form the major parts of the ubiquitous calc-alkaline batholiths.

We model 'full' or 'complete' assimilation as occurring by complete mixing of two melts. To do this we assume that the crustal material is heated above its solidus by the mantle-derived magma and then assimilated. If assimilation occurs by some process of reaction rather than direct melting then the resulting degree of assimilation will be greater than that calculated here. Furthermore, the restitic material left over in the crustal rocks after partial melts have been removed may complicate the bulk-rock geochemical signal of magma mixing on length scales determined by the size of crustal fragments.

The results are presented graphically and permit direct comparison of the thermally regulated AFC path with estimates of degrees of assimilation and crystallization obtained from geochemical mass balance. The comparison provides complementary information that can help to reveal whether a mantle-derived magma interacted with crustal rock types observed in the field, whether a mantle-derived magma interacted during ascent with an unexposed lower-crustal component, whether the assimilation occurred early or later in the local magmatic history, whether the country rocks were preheated or not, and what type of parental magma composition was involved as one end-member of the mixing process.

Geochemical estimation of the degree of assimilation of crustal rocks in calc-alkaline intrusions

Calc-alkaline rock sequences usually show geochemical characteristics of both the upper mantle and various crustal rocks (e.g. Gill, 1981). By assuming that the geochemical signatures of crustal contamination in mantle-derived magmas are the product of an AFC process, the relative masses of assimilation have been calculated using a mass-balance approach for both isotopes and trace elements (e.g. DePaolo, 1981; Aitcheson & Forrest, 1995; Bohrson & Spera, 2001; Spera & Bohrson, 2001). One difficulty of geochemical modelling of AFC processes is that the composition of the crustal assimilate, and in many cases of the parental mantle-derived magma (assimilant), is poorly constrained (see Taylor, 1980; Roberts & Clemens, 1995). Other complicating factors in AFC modelling are potential chemical modification of parental magmas in or near the mantle source (e.g. Kelemen *et al.*, 1990; von Blanckenburg *et al.*, 1992), and selective assimilation (e.g. Watson, 1982; Lesher, 1990). Despite such problems, systematic semi-quantitative patterns of assimilation have been documented at regional scales (e.g. Del Moro *et al.*, 1983*a*, 1983*b;* Pankhurst *et al.*, 1988), and for the different stages of differentiation of calc-alkaline magmas (e.g. Kagami *et al.*, 1991; Barth *et al.*, 1995; Reiners *et al.*, 1996). Because contamination is often already evident in basic members of some differentiation series (e.g. Del Moro *et al.*, 1983*a*), assimilation during the early stages of fractionation may be particularly important. In other cases the degree of assimilation seems to increase during the differentiation history (e.g. Mantovani & Hawkesworth, 1990; Kagami *et al.*, 1991).

The thermal aspects of the interaction of magmas with their host rocks will ultimately govern the amount of assimilation that is possible, and these aspects have generally not been examined in geochemical studies of AFC processes. However, thermal models of basaltic underplating (e.g. Huppert & Sparks, 1988; Bergantz, 1989) can be used to constrain the extent of crustal melting (induced by the heat released from crystallizing a basaltic sill, intruded at high temperature into lower-crustal rocks close to their melting point).

In this paper, we look at assimilation both from thermal and geochemical viewpoints, using a static mixing approach to assess both budgets, and find that useful geological information about the magmatic history, not obvious from either study alone, can be deduced.

Thermal processes during the interaction of mantle-derived magmas and crustal rocks

A very important aspect of the interaction of the mantle-derived magma and crustal rocks is the quantity of the heat released by the fractionating magma as manifest by its crystallization behaviour over its cooling interval. This heat is partitioned between 'sensible' heat, related through heat capacity to the cooling of magma and crystals (the 'heat-content' type of 'enthalpy'), and the latent heat of crystallization. Which of these two terms predominates at various stages of the cooling history determines the relative efficiency of assimilation relative to the degree of crystallization. If the multicomponent path of cotectics on the liquidus (liquid line of descent) is not affected by the assimilation, then the mass of crystals and the concomitant heat released can be deduced from phase diagrams in simpler systems (Bowen, 1922*a*, 1922*b*). More complete thermodynamic models (Nicholls & Stout, 1982; Ghiorso, 1985; Ghiorso & Kelemen, 1987: Reiners *et al.*, 1995, 1996) have shown that the liquid line of descent can in some cases be modified by assimilation.

The type of magma interaction may vary even within one intrusive complex. Although mantle-derived magma may cause melting of specific crustal rocks, in some circumstances the two melts may not mix, forming, for

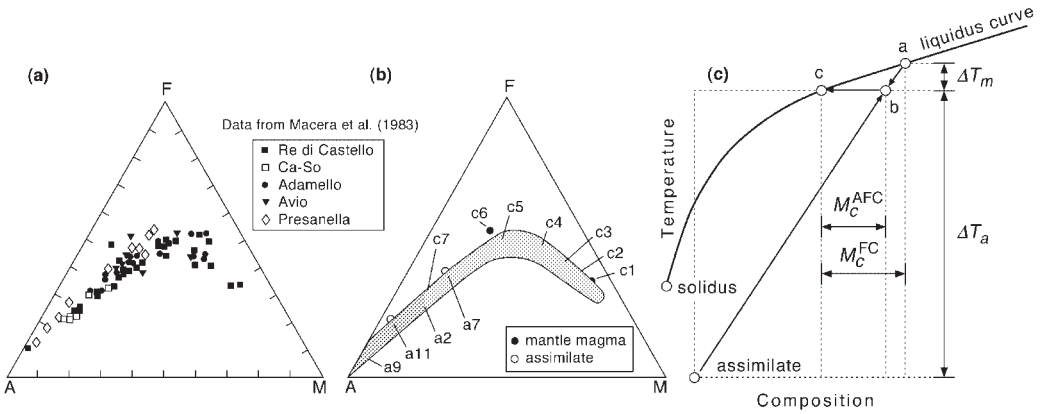

Fig. 1. (a) AFM projection [(Na_2O + K_2O)–FeO–MgO] of bulk-rock analyses from the various plutonic units of the Adamello batholith (Macera *et al.*, 1983) showing the typical calc-alkaline trend. (b) AFM projection of compositions of the various calc-alkaline dyke rocks (c1–c7 in Table 2) that could be distinct magma compositions, together with the typical compositions of the possible assimilates considered (a2, a7, a9 and a11 from Table 2). (c) Schematic pseudobinary temperature–composition diagram shows the AFM projection (or even more complicated compositional projections) onto a schematic pseudobinary temperature–composition diagram. The segment illustrated shows one step of the modelled thermal AFC process. The liquidus curve (projected liquid line of descent) relates the equilibrium composition of the melt to the magma temperature. The first stage (point a to point b) includes the cooling of the mantle magma (ΔT_m), heating and melting of the crustal assimilate (ΔT_a), and mixing of the assimilate with the mantle melt. At a second stage the supercooled hybrid melt (point b) crystallizes until it reaches the equilibrium composition (point c). M_c^{FC} and M_c^{AFC} show the difference in the mass of crystals during fractional crystallization (FC) and AFC processes.

example, layered felsic and mafic magmas. Elsewhere the two melts may mingle (become infolded) but remain unmixed on some finite scale. 'Complete mixing' here means that the two melts have chemically homogenized by mass diffusion. The first case (unmixed layers) would leave no chemical signature of melting nor assimilation. For the other two cases (mingled or completely mixed) the amount of chemical exchange measured would depend upon the size of the samples analysed. The most efficient case of 'full' assimilation is thus 'complete mixing' of the two melts resulting in chemical homogenization.

DESCRIPTION OF THE THERMAL AFC MODEL

In AFC processes, assimilation (A) and fractional crystallization (FC) are considered to occur simultaneously. The path of fractional crystallization during cooling of the melt follows the liquid line of descent in a magmatic system with many chemical components. For presentation purposes this may be viewed as the multicomponent system (Fig. 1a or b) projected onto a temperature–composition (T–X) binary diagram (Fig. 1c), or in a pseudobinary T–melt mass (T–M) binary section (Fig. 2a).

Formal description of the thermal AFC model

The formal description of the thermal AFC model can be divided in two parts: the mass balance and the heat balance. The abbreviations of the physical parameters used are explained in Table 1.

Mass balance

The AFC process was treated in the model as the sum of small AFC steps. The reference mass for the calculations of each step is the actual mass of melt M_m^i, because it determines the mass of crystallization. The mass of melt after the step i relative to its mass before depends as

$$\frac{M_m^{i+1}}{M_m^i} = \frac{M_m^i + M_a^i - M_c^i}{M_m^i} \qquad (1)$$

on the crystallized and assimilated mass. The actual mass of melt relative to the initial mass of melt is calculated from the results of all previous steps by

$$\frac{M_m^i}{M_m^0} = \frac{M_m^1}{M_m^0} \cdot \frac{M_m^2}{M_m^1} \cdots \frac{M_m^{i+1}}{M_m^i} = \prod_0^{i-1} \frac{M_m^{i+1}}{M_m^i}. \qquad (2)$$

The influence of the assimilation on the mass of crystallization was calculated with the slopes S^i in Fig. 6b by

$$\frac{M_c^i}{M_m^i} = \frac{M_c^{i^o}}{M_m^i} \cdot \left(1 + S^i \frac{M_a^i}{M_m^i}\right). \qquad (3)$$

The calculations refer to the mass of melt, but the mass of crystals and restites resulting from previous AFC steps

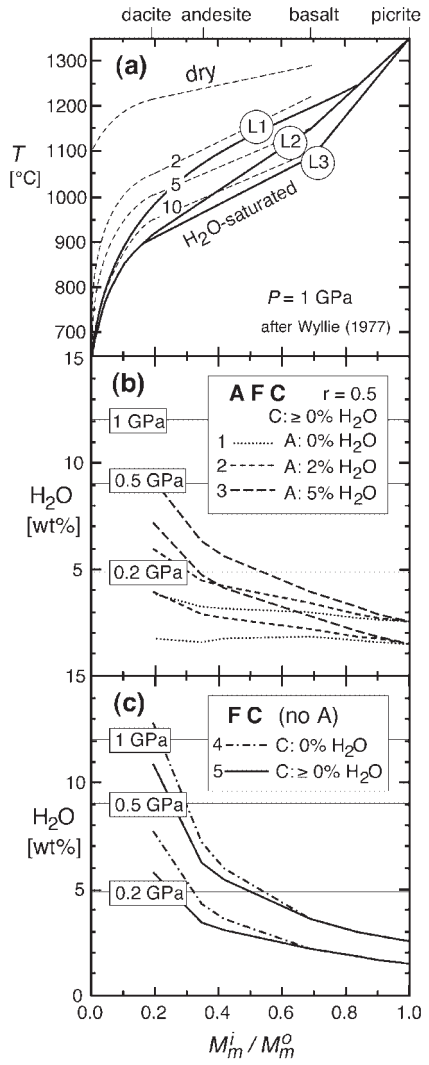

Fig. 2. Possible liquidus curve for calc-alkaline magmas shown in a temperature–composition diagram. The composition of the magma is characterized by the relative mass of magma normalized to the mass of the parental picritic magma as a result of the fractionation model M^i_m/M^0_m (see Table 1). (a) The liquidus curves used in the thermal AFC model, and experimental liquidus temperatures for various water contents at 1 GPa, are based on Wyllie (1977). (b) The water content of the melt during the AFC process, for the case $r = M^i_a/M^i_c = 0{\cdot}5$ and water contents of the crustal assimilate of 0 wt % (1, dotted line), 2 wt % (2, short-dashed line) and 5 wt % (3, long-dashed line). The initial water content of the parental melt is taken to be 1·5 (lower curves for each pair) or 2·5 wt % (upper curves). (c) The water content of the melt during fractional crystallization (FC) of (4) anhydrous phases and of (5) the phases tabulated in Table 1. The horizontal lines in B and C (labelled 0·2, 0·5 and 1 GPa) mark the maximum H_2O content of granitic liquidus melts at these pressures [as estimated by Wyllie (1977)].

can influence the heat balance. The total mass of the melt, of the crystals and of the restites is

$$M^i_{\rm tot} = M^0_{\rm m} + \prod_1^i f^{-1}.M^i_{\rm a}. \qquad (4)$$

Assuming that the crystals are fractionated not only chemically, but also physically, the total mass of magma can be formulated as

$$M^i_{\rm tot} = (1 + \varphi_x).M^i_{\rm m} \qquad (5)$$

where φ_x is the solid fraction in the magma, which is controlled in nature by magma dynamic processes. In the thermal AFC model, φ_x is given by the definition of the dimensions of the thermal system.

Heat balance

Thermal AFC processes are balanced by the heat released by the magma and by the heat for assimilation. Both involve the latent heat of crystallization and the heat for the temperature changes. The heat from cooling of the melt

$$\Delta H^{\rm liq}_{\rm m} = B.M^i_{\rm m} = c_{\rm m}.\Delta T_{\rm m}.M^i_{\rm m} \qquad (6)$$

and the heat of crystallization

$$\Delta H^{\rm fus}_{\rm m} = M^i_{\rm c}.L_{\rm m} \qquad (7)$$

are the contributions to the heat released by the mantle magma in one AFC step. The contribution from cooling the crystals can be calculated analogous to equation (6) with masses calculated in equation (4), or equation (5), or equation (7). The heat for assimilation can be formulated as

$$\Delta H^i_{\rm a} = A.M^i_{\rm a} = [f^{-1}.c_{\rm a}.(T^i_{\rm m} - T^0_{\rm a}) + L_{\rm a}].M^i_{\rm a} \qquad (8)$$

for an assimilate of melt fraction f. The heat balance between the heat for assimilation equation (8), and the heat released by the magma, equations (6) and (7), can be formulated as

$$\frac{M^i_{\rm a}}{M^i_{\rm m}} = \frac{B}{A} + \frac{L_{\rm m}}{A}.\frac{M^i_{\rm c}}{M^i_{\rm m}}. \qquad (9)$$

The substitution of equation (3) in equation (8) leads to a new formulation of the heat balance:

$$\frac{M^i_{\rm a}}{M^i_{\rm m}} = \left(\frac{B}{A} + \frac{M^{i^0}_{\rm c}}{M^i_{\rm m}}.\frac{L_{\rm m}}{A}\right) \Bigg/ \left(1 - \frac{M^{i^0}_{\rm c}}{M^i_{\rm m}}.\frac{S^i.L_{\rm m}}{A}\right). \qquad (10)$$

Procedure

For the thermal model presented here, the AFC process has been divided into small steps (i), that are characterized by a temperature interval ($\Delta T_{\rm m} = 10°$C) of the cooling mantle-derived magma. Figure 1c shows schematically one such AFC step in a pseudobinary T–X section containing the liquidus curve.

Table 1: Physical parameters, their values and some definitions of the thermal AFC model

M_a^i, M_c^i	assimilated and crystallized masses during AFC step *i*
$M_c^{i^0}$	crystallized mass during step *i* without any influence by assimilation
M_m^i	mass of the mantle melt before step *I*
M_m^{ai}	mass of the mantle melt after the hybridization with the assimilate (i.e. $M_m^i + M_a^i$)
M_m^0	mass of the parental mantle magma
M_{tot}^i	sum of M_m^0 and the assimilated masses during all previous AFC steps
T_m^0	temperature of the parental mantle magma (1350°C)
T_m^i	temperature of the mantle magma after step *i* (900–1350°C)
DT_m	temperature interval of one AFC step (10°C)
T_a^0	ambient country rock temperature (200–800°C)
T_a^s	segregation temperature of the assimilate (e.g. 900°C)
c_a, c_m	heat capacities of assimilate and assimilant (1·0–1·2, 1·3–1·5 kJ/kg K)
L_a, L_m	latent heats of crystallization (0·2–0·5 MJ/kg, Figs 3a and 4)
f	melt fraction (weight) in the country rock
φ_x	fraction of crystals in the magma
S_i	factor to account for the influence of assimilation on crystallization ($\pm$ 3)
ΔH_a, A	heat of assimilation, $A = \Delta H_a/M_a$ (0·4–4·7 MJ/kg, Fig. 3)
ΔH_m^i, B	heat released by the mantle magma in one fractionation step, $B = \Delta H_m^i/M_m^i$ (25–50 kJ/kg, Fig. 3b)
ΔH_m^{fus}, A	latent heat of fusion of the mantle magma (10–20 kJ/kg, Fig. 3b)
ΔH_m^{liq}, A	heat contribution to ΔH_m^i from cooling the mantle melt (12–15 kJ/kg, Fig. 3b)
ΔH_m^{xtal}, A	heat contribution to ΔH_m^i from cooling the crystals in the mantle magma (0–10 kJ/kg, Fig. 3b)
r	ratio of assimilated and crystallized masses, i.e. $r = M_a/M_c$
F, F'	relative mass of mantle melt, i.e. $F = M_m^i/M_m^0$, or change of mass of mantle magma in one AFC step, i.e. $F' = M_m^{i+1}/M_m^i$

The liquidus curve (liquid line of descent) relates the equilibrium composition of the melt to the magma temperature. A first stage (point c to point b in Fig. 1c) includes the cooling of the magma (ΔT_m), heating and melting of the crustal assimilate (ΔT_a), and mixing of this assimilate with the mantle melt to give a hybrid composition. At a second stage the supercooled hybrid melt (point b) crystallizes until it reaches the equilibrium composition (point c) on the liquidus surface. M_c^{FC} and M_c^{AFC} show the difference in the mass of crystals during fractional crystallization (FC) compared with AFC processes.

Our model is formulated in terms of static heat balance and aims to constrain the maximum extent of assimilation in calc-alkaline differentiation series. This means that the results are independent of the size and shape of the magma body and of kinetic aspects.

The terms 'assimilate' (e.g. Ghiorso & Kelemen, 1987) and 'assimilant' (e.g. Grove *et al.*, 1988) have both been used to denote the material that has been assimilated. Here the term 'assimilate' is used to denote the crustal melt that will become assimilated. The term 'assimilant' is used here (by analogy with the terminology for 'desiccant') to denote the magma that does the assimilation.

The limitations of the AFC process arising from mixing the assimilant (mantle-derived magma) and the assimilate (crustal melt) in the hybrid melt are difficult to constrain and are not considered further in this model. The thermal conditions for mixing are included, but dynamical aspects of mixing [such as those discussed by Sparks & Marshall (1986), Koyaguchi (1990), McLeod & Sparks (1998) and Koyaguchi & Kaneko (1999)] have not been considered. The influence of the water content of mantle-derived magmas and the melting behaviour (melt fraction vs temperature) of crustal rocks are two aspects that we wish to explore.

A fractionation model for generation of calc-alkaline magmas from hydrous mantle picrite

We have tested our thermal model for AFC processes in hydrous, mantle-derived magmas on two plutonic rock series for which we have independent estimates of the degree of crustal contamination based on geochemical data. Associated rock types in the calc-alkaline plutonic series of the Adamello batholith (Table 2; Ulmer, 1986; Matile, 1996) were used to develop a fractionation model (Table 3). Several generations of dyke rocks (Del Moro *et al.*, 1983*a*) cut this batholith, and isotopic measurements for Sr, O and Nd (Kagami *et al.*, 1991) show which of

these have no, or minor, contamination by crustal rocks. Thus the analyses for dyke rocks used here (Table 2, analyses c1–c7) are presumed to represent separate successive magma batches, which have suffered no contamination, and thus are regarded as pure-FC dykes. These dyke compositions, together with the compositions of phenocrysts that have fractionated from the dyke magmas (Table 3), have been used to calculate a fractionation model with various steps by means of the least-squares program PETMIX from Wright & Doherty (1977).

The calculation of the fractionation model follows stepwise a melt composition to the next level by mass balancing with phenocryst phases of measured composition. Two reference points are important to constrain in the fractionation models. The first is the composition of the unit amount of parent magma (M^0_m) and the second is the composition and amount of the differentiated melt before the next fractionation step (M^i_m). Our fractionation model from a hydrous picrite parent (Matile, 1996; Matile *et al.*, 2000) gives the relative magma masses related to magma compositions, down the liquid line of descent during fractional crystallization. This is our reference model for FC without A.

To calibrate the temperature and compositional evolution of the liquid line of descent from the fractionation model we have used results from experiments on hydrous mantle assemblages at specific T, P and fO_2, where the compositions of melts and crystals were measured (Ulmer, 1989). Because the relative magma mass M^i_m/M^0_m (actual magma mass normalized to initial mass of parent mantle magma) is more important than compositional variables for thermal models, the liquidus curve is most usefully presented in a T–M^i_m/M^0_m diagram (i.e. the pseudobinary section in Fig. 2a). The liquidus temperatures corresponding to magma compositions are strongly dependent on the water content (see Fig. 2b) of the magma (e.g. Wyllie, 1977).

We have considered the continental crust to be represented by a multicomponent eutectic, which in the molten state mixes with the mantle magma with no further lowering of eutectic temperature. In its general form our model for the assimilant shows some similarities to the model of Raia & Spera (1997), who considered crustal material to be a eutectic mixture. The phase diagram (Fig. 2a, relating melt fraction to temperature) is similar to that used by Barboza & Bergantz (1997), except that we have used a smoothed rather than stepped liquidus. Our phase diagram (Fig. 2a) is similar to the experimentally determined one of Johnston & Wyllie (1988), who interacted granitic with hydrous basaltic magmas at 10 kbar.

The water content of the melt is not constant during differentiation because of fractionation of amphiboles and other minerals, and because of assimilation (as shown in Fig. 2b and c). The water content is generally lowered through dilution during assimilation compared with pure fractionation, because water contents in calc-alkaline mantle magmas are higher than those of the relevant crustal rocks (e.g. Ulmer, 1989; Sobolev & Chaussidon, 1996).

The melt fraction in the melted crustal rocks

The melt fraction generated in crustal rocks at a given temperature is related to the rock's fertility; fertile rocks have mineral proportions close to the eutectic and thus higher melt fractions result for a given increment in temperature (e.g. Bergantz, 1990; Thompson, 1996). If no free water exists in the deep crust, dehydration-melting of hydrous minerals is the likely mechanism for the melting of crustal rocks that bear such phases. The reviews of experimental melting curves by Bergantz & Dawes (1994) and Gardien *et al.* (1995) show that most crustal rock types at 1 GPa ($\sim$35 km) begin dehydration melting around 800°C and reach their liquidi around 1200°C. The melt fraction curves are not linear with temperature and show two or more distinct regimes, with high melt fractions being produced in small temperature intervals and then smaller melt fractions over larger temperature intervals (a generally similar trend to the form of the T–melt mass diagram in Fig. 2a).

If the mantle-derived magma is saturated with water and this is released to the surroundings then the degree of melting of the crustal rocks will increase dramatically because of the effect of H_2O on lowering their solidus temperatures. However, for increased melting of the crustal rocks to occur, the water must be released in regions of the crust where the temperature is already high enough for melting. Water saturation in ascending magmas is normally reached only at shallow depths. In the shallow crust, assimilation hardly occurs because large amounts of magmatic heat are needed to heat the country rocks from the low ambient temperature of typical geotherms. Furthermore, the water content of the magma is in turn regulated by assimilation.

HEAT BALANCE OF AFC PROCESSES

Our model for heat balance includes both 'sensible' heat associated with temperature differences and the latent heat of crystallization. The heat of mixing of the two melts during assimilation has not been included in the heat balance, because this is a small value compared with the other contributions (Russell, 1990). The values of the heat capacity for mineral phases were calculated using the functions of Berman & Brown (1985). The values of the heat capacity for the melt phase were

Table 2: Composition of the calc-alkaline dyke rocks (c1–c7), phenocrysts and assimilates (a2, a7, a9 and a11)

	c1	c2	c3	c4	c5	c6	c7	a2	a7
SiO_2	47·54	48·85	50·20	51·39	55·47	59·34	69·97	69·30	72·31
TiO_2	0·73	0·67	0·69	0·70	0·72	0·56	0·34	0·60	0·59
Al_2O_3	13·31	15·01	15·86	17·93	19·06	18·92	15·94	17·20	15·30
FeO	9·42	8·69	8·43	8·34	7·08	6·51	2·67	2·40	2·93
MnO	0·17	0·17	0·16	0·12	0·13	0·10	0·10	0·00	0·06
MgO	16·43	13·00	10·31	7·23	3·81	2·38	1·10	1·60	0·87
CaO	10·33	11·38	11·83	10·52	8·82	8·06	4·04	1·70	3·76
Na_2O	1·25	1·80	2·16	2·54	3·08	2·77	3·15	3·50	3·05
K_2O	0·45	0·57	0·59	0·58	1·25	0·84	2·40	3·70	0·96
Cr_2O_5	0·15	0·08	0·06	0·04	0·01	0·01	0·00	0·00	0·00
NiO	0·05	0·02	0·01	0·01	0·00	0·00	0·00	0·00	0·00
Total	99·63	100·14	100·30	99·40	99·43	99·49	99·71	100·00	99·83

	a9	a11	ol_1	ol_2	ol_3	sp_1	sp_2	sp_3	cpx_2
SiO_2	75·40	72·70	41·01	39·82	39·82	0·26	0·26	0·00	51·66
TiO_2	0·15	0·45	0·01	0·00	0·00	0·40	0·40	0·37	0·39
Al_2O_3	13·50	14·90	0·02	0·01	0·01	13·03	13·03	11·75	3·87
FeO	0·64	1·70	8·61	10·97	10·97	26·43	26·43	26·03	4·73
MnO	0·04	0·11	0·14	0·39	0·39	0·42	0·42	0·60	0·10
MgO	0·10	0·54	49·67	48·44	48·44	11·96	11·96	10·93	15·80
CaO	1·00	1·63	0·14	0·19	0·19	0·03	0·03	0·02	22·82
Na_2O	4·00	2·16	0·00	0·00	0·00	0·01	0·01	0·00	0·21
K_2O	4·60	5·76	0·00	0·00	0·00	0·02	0·02	0·00	0·00
Cr_2O_5	0·00	0·00	0·00	0·02	0·02	47·26	47·26	50·24	0·42
NiO	0·00	0·00	0·29	0·14	0·14	0·19	0·19	0·07	0·00
Total	99·43	99·95	99·89	100·00	99·98	100·01	100·01	100·01	100·01

	cpx_3	cpx_4	hb_4	hb_5	hb_6	pl_4	pl_5	pl_6	$mt_{5,6}$
SiO_2	51·72	51·19	42·91	42·41	46·40	46·18	45·72	49·35	0·00
TiO_2	0·37	0·42	2·23	1·65	0·85	0·04	0·01	0·03	3·92
Al_2O_3	3·98	3·70	13·12	14·48	9·38	33·77	34·31	32·20	0·83
FeO	4·49	5·48	12·22	11·06	16·86	0·76	0·45	0·18	94·53
MnO	0·08	0·12	0·18	0·15	0·66	0·01	0·01	0·01	0·62
MgO	15·72	16·16	14·86	14·89	11·65	0·15	0·01	0·05	0·00
CaO	22·88	22·30	11·78	12·48	12·22	17·51	18·27	15·34	0·04
Na_2O	0·21	0·24	2·37	2·42	1·07	1·45	1·20	2·74	0·00
K_2O	0·00	0·00	0·29	0·43	0·92	0·12	0·02	0·11	0·01
Cr_2O_5	0·53	0·40	0·03	0·03	0·00	0·00	0·00	0·00	0·02
NiO	0·01	0·00	0·00	0·00	0·00	0·01	0·01	0·00	0·03
Total	99·99	100·01	99·99	100·01	100·01	100·00	100·00	100·01	100·00

The compositions (wt %) of the calc-alkaline dyke rocks (c1–c7) and of the phenocrysts (sp, spinel; ol, olivine; cpx, clinopyroxene; hb, hornblende; pl, plagioclase; mt, magnetite; grouped by sample numbers for the various dyke rocks) were determined by X-ray fluorescence (Ulmer, 1986) and electron microprobe (this study), respectively. These analyses form the basis of the fractionation model, together with the compositions of the assimilates used for the calculations: a2 (pelite, Vielzeuf & Holloway, 1988); a7 (amphibolite, Beard & Lofgren, 1991); a9 (biotite granite, Wyllie, 1977); a11 (biotite gneiss, Patiño Douce & Beard, 1995).

Table 3: Results of the fractionation model obtained using the least-squares program PETMIX (Wright & Doherty, 1977) and the rock and mineral analysis given in Table 2

Composition	Melt	sp	ol	cpx	hb	pl
(1) picrite	100					
		0·17	9·68			
(2) Mg-tholeiite	90·15					
		0·04	5·88	0·69		
(3) ol-tholeiite	83·55					
			3·17	11·25		
(4) basalt	69·22					
				3·36	19·08	5·00
(5) bas. andesite	41·78					
		0·10			5·17	1·55
(6) andesite	34·96					
		1·08			5·18	9·17
(7) dacite	19·52					

The relative mass of differentiated melt during fractional crystallization (normalized to the mass of primary melt) is shown with the amounts of phenocryst phases spinel (sp), olivine (ol), clinopyroxene (cpx), hornblende (hb), plagioclase (pl) and magnetite (mt) that have crystallized from each batch of fractionated melt.

calculated after the model of Lange & Navrotsky (1992), with FeO/Fe_2O_3 corresponding to the NNO (nickel–nickel oxide) oxygen buffer calculated after Kress & Carmichael (1991). The temperature dependence of the latent heat of crystallization was calculated as described by Lange & Carmichael (1990), with values from Navrotsky *et al.* (1989) and Lange *et al.* (1990), and values cited by Richet & Bottinga (1986). Because an experimental value for hornblende is not available, the latent heat of crystallization for the dehydration-melting process was approximated as the latent heat of crystallization of the normative anhydrous mineral assemblage (plagioclase and pyroxene) plus H_2O as a melt component.

Heat released by the fractionating mantle-derived magma

Because the mass of magma varies as it differentiates or assimilates crust, the heat that it releases has been normalized to the mass of parental magma as $\Sigma\Delta H^i_m/M^0_m$ (Fig. 3a), or to the mass before each AFC step as $\Delta H^i_m/M^i_m$ (Fig. 3b). The latent heat of crystallization of the magma is calculated as an average, weighted with the relative crystallized masses of each of the mineral phases formed in one fractionation step of a fixed cooling interval ($\Delta T = 10$°C) in the phase diagram of Fig. 2.

The heat capacity of the mantle melt is generally higher than that of crystals, with values decreasing from 1·5 (kJ/kg K) for the parental picritic melt to 1·2 (kJ/kg K) for granitic compositions. The contribution of the cooling of the crystals to the local heat balance depends on how efficiently they are removed from the magma. In nature, this is dependent on the magma dynamics and rheology (e.g. Marsh & Maxey, 1985). In the thermal AFC model the system is open to the inputs of crustal components (assimilates and restites) and to the output of the fractionated crystals. In our models the heat effect of cooling of separated crystals becomes significant below 1100°C (Fig. 3b, curves c and d) and is assigned to the cumulates.

Heat of melting for assimilation of crustal rocks

Three main parameters influence the heat budget for assimilation (see Fig. 4): (1) the initial temperature of the crustal rocks T_a^0; (2) the composition of the crustal melt (assimilate) relative to the liquid line of descent (Fig. 2a); (3) the temperature of segregation of the assimilatable melt T_a^s from the restite.

The fertility (which controls the crustal melt fraction at a given temperature) has a strong influence on the heat required for assimilation because both the partial melt and the restite have to be heated, but only the melt can be assimilated. The heat for assimilation has been normalized to the mass of assimilate (the crustal melt) and thus the amount of heat needed for the temperature change is inversely proportional to the melt fraction [see equation (8)]. The fertility has a much larger effect on the heat budget (see Fig. 4a and b) compared with the latent heat of crystallization (Fig. 3). Our calculations [Fig. 4, and Figs 7 and 9 (below)] consider two possible crustal rock compositions with experimentally determined melting curves: a less fertile tonalitic composition (Rutter & Wyllie, 1988) and a more fertile pelitic composition (Vielzeuf & Holloway, 1988).

Although the temperature of segregation of the partial melt from the crustal rock can be lower than the actual temperature of the hybridizing magma, assimilation is most efficient if both segregation and assimilation occur at the same temperature (compare the cases $T_a^s = T_a^i$ with $T_a^s = 900$°C in Fig. 4).

The initial country rock temperature T_a^0 is represented in our calculations by a range from upper-crustal values

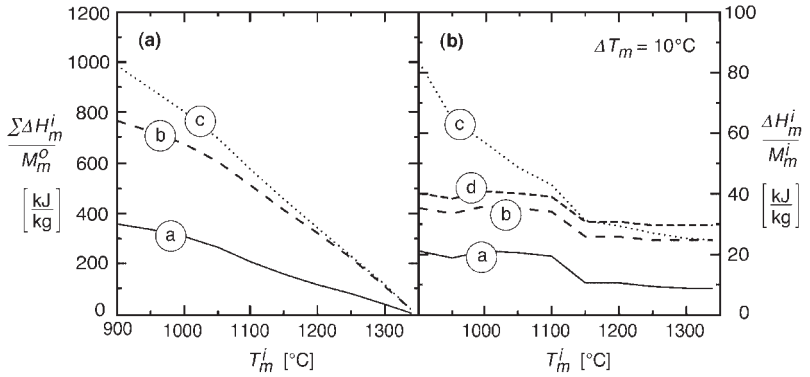

Fig. 3. (a) Heat released by the mantle magma over the temperature interval as the sum of all previous AFC steps normalized to the initial mass of magma ($\Sigma\Delta H^i_m/M^0_m$). (b) Heat released during each AFC step (ΔT_m = 10°C) normalized to the actual mass of magma ($\Delta H^i_m/M^i_m$). The contributions to the total released heat of the latent heat of fusion ΔH^{fus}_m for the given mineralogy spread over the supersolidus region, the cooling of the melt ΔH^{liq}_m and the cooling of the crystals ΔH^{xtal}_m are labelled as (a) ΔH^{fus}_m, (b) $\Delta H^{fus}_m + \Delta H^{liq}_m$ and (c) $\Delta H^{fus}_m + \Delta H^{liq}_m + \Delta H^{xtal}_m$; (d) assumes for ΔH^{xtal}_m a fixed crystal fraction in the magma of 0·3. The kinks in the curves of (b) reflect the steps of the fractionation model (Table 1).

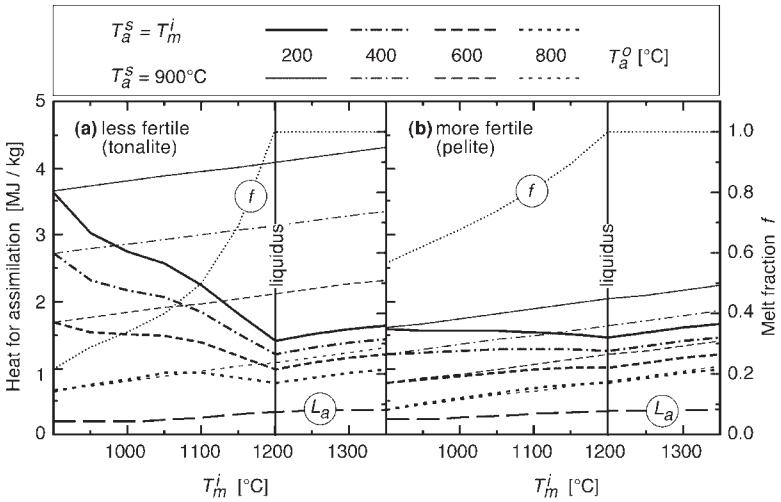

Fig. 4. Heat for assimilation of crustal rocks $\Delta H_a/M_a$ as a function of the magma temperature T_m. The initial temperature of the crustal rocks T^0_a varies between 200 and 800°C. The melt fraction f as a function of temperature is drawn as a measure of the fertility of rocks to melting. (a) The tonalite experimentally studied by Rutter & Wyllie (1988) represents a rock type of low fertility. (b) The pelite studied by Vielzeuf & Holloway (1988) represents a fertile rock type. Bold lines represent the country rocks that achieve the magma temperature T^i_m, e.g. assimilation of small xenoliths, which become heated to the magma temperature ($T^s_a = T^i_m$). Fine lines originating at 900°C represent the case where the crustal melt (assimilate) is segregated at a particular temperature of T^s_a = 900°C out of the country rock. The latent heat of fusion L_a is small compared with the total heat of assimilation.

of 200°C to values of 800°C, more typical for orogenically active lower crust. For specific geotherms, initial crustal temperatures can be easily related to particular crustal depths. Temperatures of 800°C could represent a 'Moho region' that has been preheated by previous passage of mantle magma batches, whereas 400°C is more characteristic for non-orogenic lower continental crust. Higher initial country rock temperatures caused by basaltic underplating will lead to extensive lower-crustal melting. If these non-cogenetic crustal magmas solidify before the next pulse of mantle magma then they cannot participate in AFC processes.

MASS BALANCE CONSTRAINTS ON AFC PROCESSES

Because our thermal model is formulated to be independent of the size of the magma body, the results of the calculations are expressed as relative masses of

crystallization and assimilation. These relative masses can be referred to different reference masses (e.g. appropriate to lengths of specific plutons or sills) when compared with particular field examples.

Graphical representation of masses involved in AFC processes

A crystallization vs assimilation plot (C–A plot, Fig. 5) is used in two different ways: (1) the total crystallized and assimilated masses are normalized to the initial mass of parental mantle magma in the $\Sigma M^i_c/M^0_m$ vs $\Sigma M^i_a/M^0_m$ plot (see Fig. 5). The contours labelled *F*, and characterized with a slope of one, represent the mass of melt relative to the initial mass of parental mantle magma. (2) The actual masses crystallized and assimilated in one AFC step are normalized to the mass of melt before the AFC step (i.e. M^i_c/M^i_m and M^i_a/M^i_m). This plot represents the direct result of the calculations of one AFC step, independently of what happened before. The results in this plot are characterized by the ratio of assimilation and crystallization, $r = M^i_a/M^i_c$, and *F* can be interpreted as the change of magma mass during one AFC step, i.e. $F' = M^{i+1}_m/M^i_m$.

The results of our thermal models are overlaid onto C–A plots in later figures to illustrate how the relations between rock types and temperature in the fractionation series can be related to values of *r* and *F* deduced from geochemical measurements and modelling.

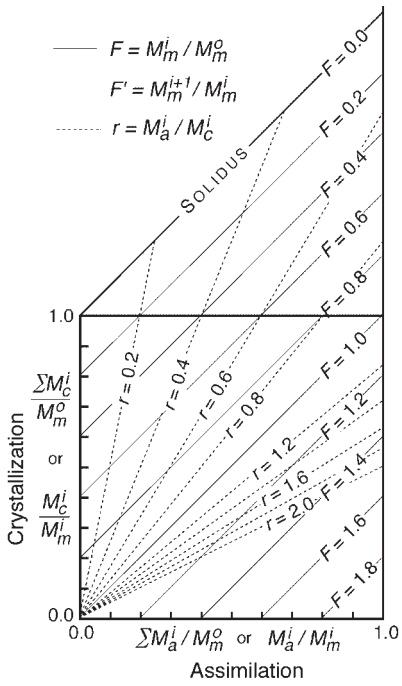

Fig. 5. Two types of crystallization vs assimilation (C–A) diagrams, normally used to interpret geochemical data, are superimposed and used to represent the results of the thermal AFC models. (1) The sum of the crystallized and assimilated masses is normalized to the initial mass of mantle magma in a $\Sigma M^i_c/M^0_m$ vs $\Sigma M^i_a/M^0_m$ plot. The relative magma mass $F = M^i_m/M^0_m$ is shown as continuous lines with a slope of unity parallel to the line labelled SOLIDUS. (2) The masses that are crystallized and assimilated in one AFC step are normalized to the mass of mantle melt before this AFC step in an M^i_c/M^i_m vs M^i_a/M^i_m plot. This plot is the direct result of the heat balance and is characterized by $r = M^i_a/M^i_c$ (dotted lines), which corresponds to the reciprocal of the illustrated slope of the diagonals to the origin ($1/r = M^i_c/M^i_a$).

Amount of crystallization and degree of assimilation

Assimilation is included in these fractionation models based upon the assumption that the liquid line of descent will not be influenced by small degrees of assimilation [see Ghiorso & Kelemen (1987) for a discussion of when the liquid line of descent will be affected, and when not]. The composition of the assimilating magmas (c1–c7) and the composition of the crustal melts (assimilates: a2, a7, a9, a11) are plotted in Fig. 1b compared with bulk-rock analyses from several units of the Adamello batholith (Fig. 1a). The effect of assimilation of 'granitic' crustal melts on the mass of crystallization of the fractionating hydrous mantle-derived magma has been calculated modifying the magma fractionation model (AFC, summarized in Table 1; Matile *et al.*, 2000), which is valid for *P* from ~0·5 to 1·0 GPa (~17–35 km) as outlined above.

During AFC processes the mass of the assimilant (mantle melt) is not constant because of open-system behaviour (fractionation of crystals occurs simultaneously with assimilation). The hybrid mass increases through assimilation (A) and decreases through fractionation of crystals (FC), with the result that the mass involved in AFC processes is greater than the mass involved in pure fractional crystallization. The mass of fractionated crystals was calculated with the assumption of a progressively changing phenocryst assemblage in the contaminated mantle-derived melt and thus a single liquid line of descent. This assumes that assimilation does not significantly change the liquid line of descent (see Ghiorso & Kelemen, 1987; Kelemen, 1990). After mixing the crustal assimilate with the mantle melt, the mass of crystals was calculated using the compositions of the hybrid melt (the next member in the differentiation sequence) and of the phenocrysts.

THERMAL LIMITS OF ASSIMILATION IN AFC PROCESSES

Some results of the calculations of the thermal AFC models are superimposed on C–A plots in Figs 6 and 7, and are represented as $\Sigma M^i_c/M^0_m$ vs $\Sigma M^i_a/M^0_m$ plots in Fig. 6a, and as M^i_c/M^i_m vs M^i_a/M^i_m plots in Fig. 6b. These

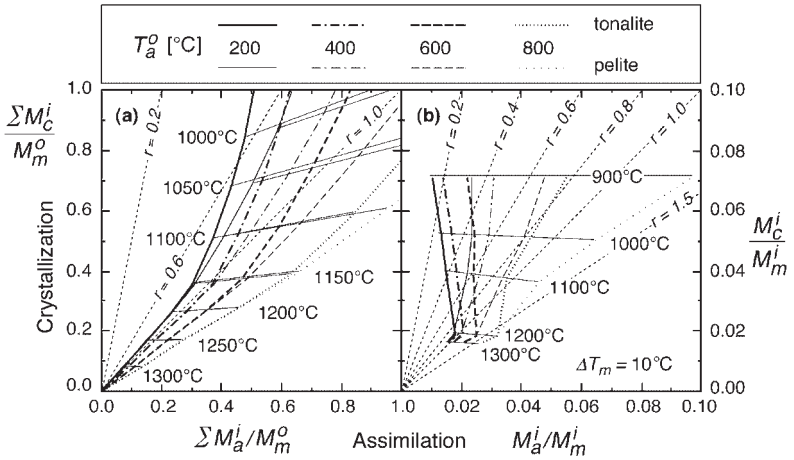

Fig. 6. Results of thermal AFC models emphasizing the importance of the initial temperature and fertility of the country rocks in the assimilation history, represented in (a) as $\Sigma M_c^i/M_m^0$ vs $\Sigma M_a^i/M_m^0$ plots, and in (b) as M_c^i/M_m^i vs M_a^i/M_m^i plots (as in Fig. 5). The scale of (b) corresponds to the temperature interval of $\Delta T_m = 10$°C in each AFC step. The initial temperature of the country rocks is 200, 400, 600 or 800°C, as shown by various line ornaments. The temperature contours show the degree of differentiation in the AFC process and are linked to magma compositions by the liquidus curve (Fig. 2a). The primary magma has a picritic composition and a temperature of 1350°C. The fertility of the assimilate is calculated for the less fertile tonalite [bold lines; *T–f* data from Rutter & Wyllie (1988)] and for the fertile pelite [fine lines; *T–f* data from Vielzeuf & Holloway (1988)]. The AFC process is treated as assimilation of small xenoliths (Fig. 4) at the magma temperature ($T_a^s = T_m^i$).

results for the AFC paths can also be read directly in terms of *r* and *F* values as shown in Fig. 5.

The closed (isenthalpic) systems considered show that the thermal limits of AFC processes are mainly controlled by the ambient (initial) temperature of the crustal rocks (reflecting the pre-magmatic environment, Fig. 6), by their composition (fertility to melt production, Fig. 6), and by the properties of the mantle-derived magma (temperature, composition, water content and crystallization interval, Fig. 7). In all cases the AFC paths are characterized by two distinct segments with distinct slopes.

Initial crustal temperature and fertility

Noticeably different types of behaviour are indicated depending upon the following:

(1) initial crustal temperature: because the crustal rocks need heat both to raise their temperature from ambient to their solidus (sensible heat) and for fusion (latent heat), the degree of assimilation of crustal rocks initially at 200°C is about half of that of crustal rocks initially at 600°C (Fig. 6a). Hotter (deeper) crustal rock temperatures in excess of 600°C (depth of 30 km for a gradient of 20°C/km) clearly lead to more efficient assimilation for deeper than for colder (shallower) crustal rocks.

(2) Fertility of crustal rocks: the *r* values in Fig. 6 are dependent much more on the initial country rock temperature than upon the fertility (as can be seen here by comparing pelite with tonalite).

Mantle-derived magma temperature and composition

Figure 6 shows also the importance of the initial magma temperature on the degree of assimilation. Higher *r* values (the slopes defining the mass ratios of assimilation to crystallization) occur for the interval 1350–1150°C (r = 1·0–1·5) compared with 1150–900°C (r = 0·6–0·2).

The mantle magma temperature, which is related to its composition, influences the heat balance by the amount of heat released in one AFC step and by the temperature at which this heat is released relative to the liquidus temperature to composition relation. The mantle magma temperature is important, because it controls the melt fraction in the crustal rocks and the maximum temperature of assimilation. The decreasing liquidus temperature during differentiation of the hybrid magma is the main reason for the decreasing assimilation potential. This is evident from decreasing *r* values in Fig. 6b along the liquid line of descent. Figure 6b clearly shows that the highest temperature interval, from picrite to basalt, is the most efficient (highest *r* values) of any assimilation step.

The water content of the hybridizing magma is of importance because it shifts the liquidus to lower temperatures and it increases the temperature interval of fractional crystallization (Fig. 2). The first effect decreases the assimilation potential through lowering of the liquidus temperature and the second effect leads to an increased total heat released by the mantle magma. The net influence of an increased water content is most visible for intermediate magma compositions at the end of the AFC

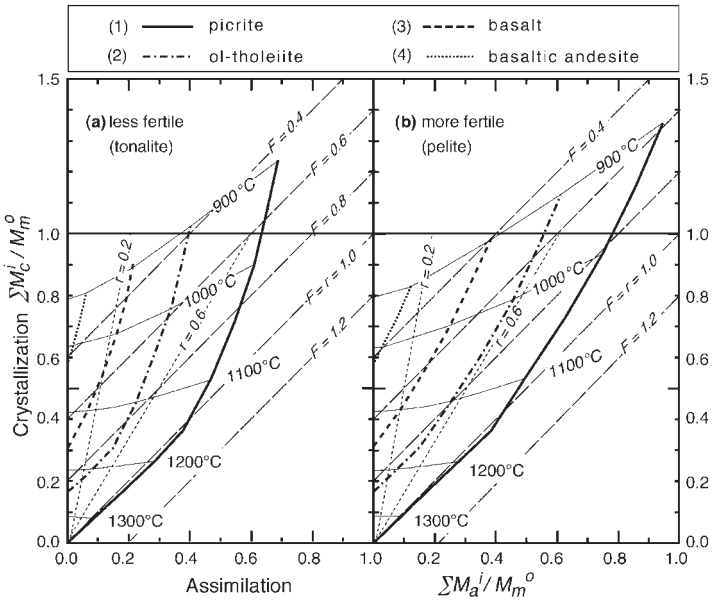

Fig. 7. Results of thermal AFC models emphasizing the beginning of assimilation of (a) tonalite and (b) pelite into the possible range of primary arc magmas. The fractionation history is represented in the $\Sigma M_c^i/M_m^0$ vs $\Sigma M_a^i/M_m^0$ plot (as in Fig. 5). The initial temperature of the country rocks considered is 400°C (from Fig. 6). The temperature contours show the degree of differentiation in the AFC process and are linked to magma compositions by the liquidus curve of Fig. 2a. Assimilation can begin at various stages in the differentiation history of the mantle magma as illustrated for picrite (1), ol-tholeiite (2), basalt (3) and basaltic andesite (4). Pure FC without A (A = 0) is represented by the left-hand axis.

process. Consequently, the assimilation potential of calc-alkaline magmas (tonalite–granodiorite) is less than that of basalt (tholeiite).

Figure 7 shows the crystallization–assimilation relationships calculated for ultrabasic to basic magmas. As can be seen in Fig. 7, the starting composition of the mantle magma for the AFC process is very important for two reasons:

(1) the decreasing assimilation potential during differentiation means that basaltic andesites (fine dotted lines at the left in Fig. 7) assimilate very little crust at advanced stages of fractional crystallization (F from 0·4 to 0·3) compared with more primitive compositions (picrite, continuous lines in the middle of Fig. 7), especially early in their history;

(2) because assimilation increases the magma mass and also the mass of the subsequent crystallization, the AFC process has to start at the very beginning of differentiation (picritic phase) to result in high degrees of assimilation.

The differences of r values (the ratio of the crystallized to assimilated masses) for the four starting examples in Fig. 7 do reflect the assumption that the liquid line of descent of the mantle magma and the assimilation path are the same, and that the crystallizing assemblage is not changed by the assimilation. In the extreme case of mixing of picritic and granitic melt this is probably not true if olivine disappears from the liquidus, and hence erroneously may result in a calculated increase in the amount of crystals (e.g. example 1, from picrite to Mg-tholeiite, in Fig. 7; see also Ghiorso & Kelemen, 1987). Even if the differences between 'down-temperature FC' and 'up-temperature A' paths can be evaluated from experiments, it still does not permit discrimination between different source compositions resulting, for example, from metasomatism in mantle source regions. More comprehensive models have recently been developed by Spera & Bohrson (2001), which can examine the behaviour of mobile elements.

Closed-system heat and mass transfer (AFC)

Melt paths have been calculated (Fig. 7) for closed-system heat and mass transfer in AFC processes, as a function of mantle magma temperature, initial crustal rock temperature (shown for 400°C in Fig. 7) and fertility (tonalite to pelite). The calculated FC paths with no A are shown by the left axis in Fig. 7 with pre-assimilation crystal contents of 18, 31 and 58% for the respective fractionation steps from hydrous picrite (1) to olivine tholeiite (2), to basalt (3), and to basaltic andesite (4; Table 3). The calculated maximum amounts of assimilation expected for rocks of lesser to greater fertility (tonalite to pelite), at various initial temperatures (200, 400, 600, 800°C), and for various stages of fractionation, are presented in Table 4. The fact that the four curves are sub-parallel,

Table 4: Maximum amounts of assimilation expected for rocks of lesser fertility (tonalite) to greater fertility (pelite) at four initial temperatures (200, 400, 600, 800°C) for various stages of assimilation, relative to 100% initial mantle magma

	ΔT°C	800°C		600°C		400°C		200°C	
		ton	pel	ton	pel	ton	pel	ton	pel
picrite	1350–900	120	130	80	105	70	80	50	65
Ol-tholeiite	1250–900	80	90	55	75	40	55	32	50
basalt	1150–900	50	60	36	52	20	40	15	30
bas. andesite	1050–900	30	40	18	30	3	12	3	8

ton, tonalite; pel, pelite.

i.e. have similar r values at different temperatures, reflects the relatively simple shape of the liquidus surface, which projects as nearly a straight line in T–X and T–M diagrams (Figs 1 and 2).

Spera & Bohrson (2001, p. 1018) have provided access to an EXCEL spreadsheet version of their program, which can be used to develop further models of the type presented here. Although they have not specifically considered assimilation of crustal rocks by hydrous mantle-derived magmas, the model of Spera & Bohrson is suitably formulated to consider any magma type as long as the physical parameters of melt fraction can be described as a function of temperature and pressure. Much more complicated AFC histories than considered here can be treated with future modifications to their model by breaking the AFC path into segments each with characteristic phase relations. The values of F and r as used here are determined as their parameters M_m/M_0 and M_a^*/M_c.

AFC IN ALPINE PLUTONS

AFC paths calculated from heat-balance constraints, or from the fractionation model (Figs 6 and 7), expressed in terms of the ratio F (final mass of magma/initial mass of magma) and r (mass assimilated/mass crystallized), can be related to AFC paths constrained by mass-balance calculations (Fig. 8). In several geochemical studies (e.g. DePaolo, 1981; Grove *et al.*, 1988; Aitcheson & Forrest, 1995) F and r are obtained by mass balancing specific elements (in particular, Rb/Sr and Nd/Sm) relative to assumed concentrations for assimilant (mantle magma) and assimilate (crustal melts).

There have been several geochemical investigations of the Alpine plutons related to the Periadriatic Lineament [Fig. 9; see also review by von Blanckenburg *et al.* (1998)], which can be used to compare the geochemically deduced amounts of AFC with the calculated amounts from the models. The few studies to date have concentrated on the Adamello intrusion, with some work on the Bergell pluton. The Adamello has a longer history (43–30 Ma, Del Moro *et al.*, 1983*b*) than the Bergell (Hansmann, 1996), which appears at the end stage (32–30 Ma) of the plutonic history.

Comparison of thermal and geochemical estimates of degree of contamination in Alpine plutons

The shaded bands in Fig. 8a between the lines c1, c3 and c4 refer to F–r ranges calculated using the fractionation models (Table 1), which lead to dacitic or andesitic rocks by differentiation of picrite (c1), olivine tholeiite (c3), or basalt (c4, Table 2). These results, from mass-balance modelling relative to our temperature–composition models, can be compared with specific values of r and F obtained from trace element and isotope modelling of particular AFC processes. Some results for samples of the Adamello and the Bergell intrusions in the Italian Alps are shown in Fig. 8b.

From their geochemical modelling for the Adamello batholith, Del Moro *et al.* (1983*a*), Bigazzi *et al.* (1986) and Kagami *et al.* (1991) obtained r values of 0·23, 0·2 and 0·6, respectively, for different intrusive suites. In addition, von Blanckenburg *et al.* (1992) obtained r = 0·5 for their samples from the Bergell intrusion. As was done by these workers, it is generally necessary to assume that r values for samples from particular localities were constant, and are associated with definite F values through the AFC modelling (de Paolo, 1981).

These 'geochemical' r and associated F values for individual samples (symbols in Fig. 8b) overlap with the fractionation-model constrained AFC paths for these magma bodies but show different degrees of assimilation

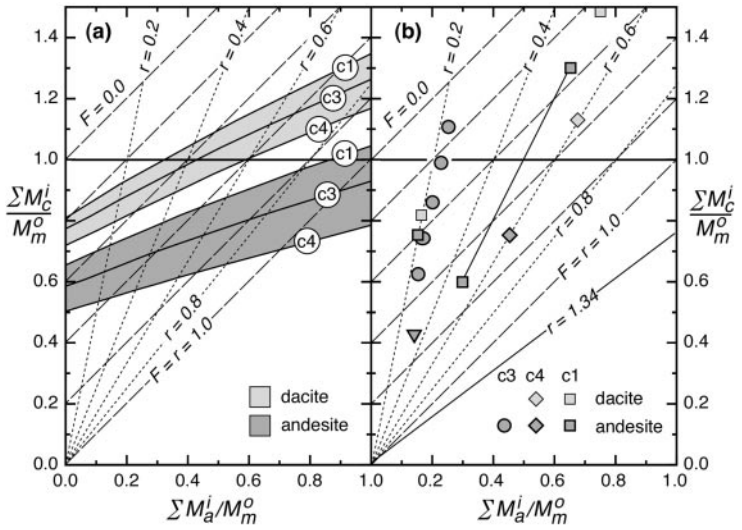

Fig. 8. Relationship between mass of crystallization to assimilation for hybrid dacitic (lighter symbols) or andesitic magmas (darker symbols) expressed as the ratios of $\Sigma M_c^i/M_m^0$ and $\Sigma M_a^i/M_m^0$. (a) Results of mass balance calculations of an AFC process with different starting compositions of the assimilant (c1, picrite; c3, ol-tholeiite; c4, basalt; Table 2). (b) The results of geochemical modelling. Data for the Adamello batholith from Del Moro *et al.* (1983*a*, $r = 0{\cdot}23$), Bigazzi *et al.* (1986, $r = 0{\cdot}2$) and Kagami *et al.* (1991, $r = 0{\cdot}6$) and for the Bergell from von Blanckenburg *et al.* (1992, $r = 0{\cdot}5$). The Adamello samples with $r = 0{\cdot}2$ are for shallow intrusions that have crystallized *in situ* into country rocks with low initial temperatures. The constant value of r is the result of choosing a single 'granite' assimilate. The samples with $r = 0{\cdot}6$ represent gabbroic rocks with a high-pressure igneous stage, or homogeneous tonalite from deep-seated magma chambers. The inverted triangle ($r = 0{\cdot}34$, $F = 0{\cdot}68$) and the line $r = 1{\cdot}34$ refers to Grove *et al.* (1988), calculated as explained in the text.

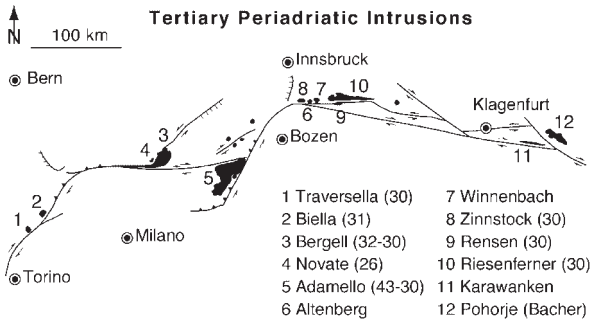

Fig. 9. Regional map of the Tertiary intrusions along the Periadriatic Lineament of the European Alps. The radiometric age of minerals from the intrusions is given in parentheses (Ma) after the summaries by Callegari (1983), Dal Piaz & Venturelli (1983), Werling (1992) and Romer *et al.* (1996).

for the different rock types involved. Some useful observations can be made from a comparison of these 'geochemical-model' F and r values with 'fractionation-model' F and r values, and with the AFC paths calculated by heat balance (Figs 6 and 7). The trend with $r = 0{\cdot}2$–$0{\cdot}23$ in Fig. 8b is consistent with assimilation of less fertile crust (e.g. tonalite) by a fractionated basaltic magma (compare with Fig. 7a), or alternatively that less fractionated (higher temperature) picritic magma assimilated fairly cold crustal materials (Fig. 6a, e.g. 200°C crustal rocks into 1350°C picrite). The latter alternative is consistent with the suggestion by Kagami *et al.* (1991, p. 14338) that the 'mafic rock series' represents contamination of a primary picrobasaltic magma by cold average crustal rocks in the early stages of an intrusion late in the magmatic sequence of the southern part of the Adamello batholith.

The trends with $r = 0{\cdot}5$ and $r = 0{\cdot}6$ could indicate assimilation of less fertile crust (e.g. tonalite) by a hotter hydrous picritic magma (Fig. 7a) or, alternatively, assimilation by a more fractionated magma (e.g. hydrous olivine tholeiite, Fig. 7b) of fertile crust already preheated to near its solidus temperature. The latter alternative is consistent with the suggestion by Kagami *et al.* (1991, p. 14340) that the 'intermediate rock series' represents contamination of hydrous gabbroic magma by heated crustal rocks at some evolved stage in the intrusive history.

In the southern Adamello, picritic dyke rocks and some gabbroic intrusions, which have undergone fractionation at shallow depths, show very minor amounts of assimilation. Surprisingly, even some tonalites show geochemical evidence of minor amounts of assimilation, and are the products of fractionation with incorporation of cumulates (Callegari & Dal Piaz, 1973; Dupuy *et al.*, 1982; Ulmer *et al.*, 1983; Blundy & Shimizu, 1991). The key control here is the low initial (<200°C) temperature of the country rocks. This is consistent with the observation that the Adamello intrusion in the south is emplaced at shallower levels than the Bergell intrusion. Petrological observations of the contact metamorphic country rocks (e.g. Ulmer, 1982; Ricklin, 1985), as well

as clinopyroxene geobarometry of gabbroic cumulates (Nimis & Ulmer, 1998) indicate pressures not in excess of 3 kbar during emplacement of the majority of the mafic to intermediate plutonic rocks in the southern Adamello. In contrast, amphibole barometry of the main tonalities of the Bergell intrusion suggests 5–7·5 kbar pressure during emplacement (Reusser, 1987), and thus initial temperatures of the country rocks are expected to have been higher here.

In the southern parts of the Adamello, there is good evidence for polybaric fractionation (first at 25–30 km, ~8 kbar) ending at shallower levels. This includes (1) two generations of clinopyroxene indicating initial crystallization at high pressure (8–10 kbar) followed by shallow-level crystallization of matrix clinopyroxene at pressures of <3 kbar (Nimis & Ulmer, 1998), and (2) plagioclase zoning pattern in cumulate gabbros, in particular for Sr and Ba [as reported by Blundy & Shimizu (1991)]. The gabbroic rocks here show practically no evidence for assimilation (e.g. Del Moro *et al.*, 1983*a*; Kagami *et al.*, 1991, samples 11, 12, 13, 14), whereas the intermediate rocks (tonalites) show intermediate amounts of assimilation. This supports the suggestions that the early magmas, even at depth, encountered crustal rocks that were far from their melting points. Earlier magma batches intruding the lower crust (a process of 'interplating') increased the heat input such that subsequent magmas could assimilate greater amounts of hotter crustal rocks during their fractionation.

The mantle-derived magmas, represented by the uncontaminated dyke-rocks, appear to have been contaminated by fertile lower-crustal rock types (granite or pelite) on the basis of $^{87}Sr/^{86}Sr$ and oxygen isotope studies (Cortecci *et al.*, 1979; Kagami *et al.* 1991), to form the Adamello batholith. Conversely, the intrusive rocks of the deeper-seated Bergell exhibit source magma (mantle) contamination involving aqueous fluid infiltration (Del Moro *et al.*, 1983*b*; von Blanckenburg *et al.*, 1992; Matile, 1996, fig 5.6, p. 150). Thus the Bergell magmas assimilated 'higher-temperature' (granulite facies) lower-crustal rocks compared with the Adamello (assimilation of amphibolite facies rocks). The Adamello rocks do indicate increased amounts of assimilation from gabbro to granite, perhaps by a factor of two (Bigazzi *et al.*, 1986; Kagami *et al.*, 1991, fig. 6, r from 0·2 to 0·4) although the modelling by these workers assumed constant r values.

The crustal thickness at the time of the Adamello intrusion is not constrained by the geochemistry. The earliest and latest magmas have the lowest amounts of assimilation and the middle ones have the highest amounts of assimilation. This suggests that the 'interplating' of earlier magmas is vital to heat up the crustal rocks before they can participate in assimilation histories, and that the late-stage picrobasaltic to basaltic dyke rocks that represent very subordinate magma volumes were intruded by a different mechanism, which did not involve a prolonged residence in a magma chamber, but which fractionated *en route* and did not induce much assimilation. It is also possible that the lower crust was exhausted of its low melting fraction by this stage.

The late Alpine intrusions (Fig. 9) were emplaced in a transpressional environment (Trümpy, 1973, 1975; Laubscher, 1983) where intrusion at deeper crustal level optimized assimilation and generation of large volumes of intermediate members of the calc-alkaline plutonic series. Assimilation in these batholiths has taken place in magma chambers deeper than the present level of observed stoping. The stoping seen in the Adamello is at the stratigraphic level of the carbonate country rocks at shallow crustal levels. These are refractory rocks when H_2O is not abundant and result in the production of calc-silicates in the contact aureoles. The highest degree of contamination in the Adamello pluton, inferred from geochemistry, occurs where the intrusion level is deepest (northwestern Adamello) and where the country rocks are fertile and hotter, and least where the country rocks are coldest and where they are dry carbonate sediments.

AFC processes in plutonic compared with volcanic series

In general, to distinguish between the compositional changes and the volumes of the various calc-alkaline rock-types being due to mostly FC or more to A, is to determine in specific field areas at which stage in the histories contamination took place. Assimilation takes place most pronouncedly at higher temperature, i.e. during earlier magmatic stages. For example, during hydrous picrite cooling from 1350 to ~1150°C much heat is released without much crystallization of olivine [Fig. 3 and Matile *et al.* (2000, fig. 4, p. 188)]. This results in a high r value (~1·5) in the models (Figs 6 and 7). If these magmas do not ascend rapidly but build magma chambers increasing the possibility of assimilation, then large amounts of intermediate members of the calc-alkaline series would result. Alternatively if mantle-derived hydrous picrites ascend rapidly and do not undergo high-temperature assimilation, then the large degrees of crystallization that occur between 1150 and 1080°C [of clinopyroxene, amphibole, then plagioclase and magnetite; Fig. 7 and Matile *et al.* (2000, fig. 3, p. 186)] will rapidly diminish the amount of residual liquid as it shifts to SiO_2-rich compositions. This suggests that in FC-dominated volcanic series the bimodal 'Daly Gap' is characteristic, whereas in AFC-dominated plutonic series larger volumes of intermediate members of the calc-alkaline series would form. Furthermore, increased pressure and water content have important effects on controlling the different crystallization behaviour of calc-alkaline magmas (Anderson, 1980; Green, 1982) in plutonic compared with volcanic settings.

In general, low-pressure, dry, T–composition sections show a step in the liquidus such that high-temperature olivine crystallization (steep dT/dX) is followed by a step where plagioclase and pyroxene $\pm$ magnetite crystallization occurs (low dT/dX, also where a large compositional shift in magma composition occurs, e.g. Grove & Baker, 1984), which in turn is followed by feldspar + quartz crystallization with steep dT/dX. This pyroxene + plagioclase $\pm$ magnetite crystallization region corresponds approximately to the 'Daly Gap', resulting in bimodal suites of mafic and felsic rock types, with few intermediate members in such fractionation sequences. At higher pressures, in the presence of H_2O, in T–composition sections (such as that in Fig. 2a), the incoming of pyroxene occurs earlier, the crystallization of plagioclase is delayed and/or replaced by amphibole (Ulmer, 1989; Sisson & Grove, 1993), so that the T–X step is lessened and appears as an inflection without the very flat dT/dX region in the middle, and thus without the 'Daly Gap'. This serves as an explanation of why the 'Daly Gap' is more common in volcanic than in plutonic rocks.

These phase relations also appear to be reflected in specific tectonic settings. In extensional settings (back-arcs and rifts) mantle-derived magmas originating by mantle decompression cool quickly at shallow depths. They either quench to basalt or reach the granite minimum by differentiation dominated by fractional crystallization. A transpressional environment (as in the Alpine convergent margin) will be characterized by slow processes of melt migration and formation of intrusions at deeper crustal level. Thus earlier magmas can preheat the country rocks to promote subsequent assimilation. Such magmas will have a long residence time in deep-seated crustal magma chambers, so that assimilation will be optimized. These simple relations between depth, cooling rate and degree of assimilation can be investigated further in future studies.

EFFECT OF THE TYPE OF THERMAL MODEL ON THE INTERPRETATION OF AFC HISTORIES

Our study is different from other recent considerations of the thermal effects of crystallization and assimilation in that we have considered hydrous picritic magma fractionation at lower-crustal depths (17–35 km). For example, Ghiorso & Kelemen (1987) investigated the thermal effects of assimilation of felsic crust by anhydrous mid-ocean ridge basalt (MORB) at low pressures, and Reiners *et al.* (1995) investigated the thermal effects of assimilation of felsic crust by anhydrous MORB and hydrous high-Al basaltic (HAB) magma. Their results produced a greatly increased value of r at the early stages of assimilation (r of 2·3–2·7), which decreased following plagioclase and pyroxene replacing olivine saturation on the liquidus. Furthermore, Reiners *et al.* (1996) considered that the H_2O to form hydrous minerals in basalt fractionates was added from the assimilated crustal rocks [as previously suggested by Patchett (1980) and Thompson *et al.* (1982)] not from the mantle magma. In our models (Fig. 2) we include both mantle H_2O and assimilated H_2O sources.

As proposed by Bowen (1922*a*, 1922*b*), and elaborated on by Ghiorso & Kelemen (1987), assimilation of felsic crust by mafic magma would result in reduction of the amount of high-temperature crystallization. This will result in r values greater than unity for assimilation in the early cooling history of mafic magma [as noted by Reiners *et al.* (1995, p. 565)]. Our models (Figs 6 and 7) generated r values greater than unity for fertile crustal compositions (pelite) at high temperatures (>600°C) being assimilated by high-temperature hydrous picrite to olivine tholeiite compositions (Matile *et al.*, 2000, fig. 6, p. 191).

Both our models and those by Reiners *et al.* (1995, fig. 3, p. 565) for MORB and HAB compositions produced an early stage of high r (up to 2·7) followed by a subsequent stage of lower r. The switchover near 1180°C in the calculations of Reiners *et al.* results from saturation with plagioclase and clinopyroxene following olivine fairly early in their calculated fractionation history (after only ~50–70°C of cooling). Our hydrous picritic magma composition produces a much smaller change in r than theirs, as hornblende and plagioclase replace clinopyroxene on the liquidus. Because the liquidus surface used for our calculations is much more continuous than those for anhydrous systems at low pressure, it shows almost a straight line in the T–M diagram, including the early segment with olivine (Matile *et al.*, 2000, fig. 2, p. 185).

Assimilation processes by our more primitive hydrous model mantle magma (picrite or olivine tholeiite) produced r values very close to unity in the earlier parts of the fractionation sequence. This occurs because in our model the sensible heat term ($M_m C_p^m \Delta T_m$) is about equal to the latent heat term ($\Delta H_f M_c$) through the interval 1350–1150°C (Matile *et al.*, 2000, fig. 4, p. 188) whereas in the MORB–HAB models of Reiners *et al.* (1995) the ratio $M_m C_p^m \Delta T_m / \Delta H_f M_c$ is very large, reflecting the particular T–X relations.

Spatial and temporal relations of AFC in other examples

The comparison of the thermal–petrological AFC paths obtained in this study with geochemically determined AFC paths [constrained by considerations of Aitcheson

& Forrest (1995)] will permit the estimation of the likely location of the depth of magma chambers in crustal columns and enable us to evaluate the mode of assimilation. This, in turn, raises the general question of how far apart in space and time FC and A can be to define a closed (isenthalpic) system. In this regard we will consider the implications of the study by Grove *et al.* (1988) for the assimilation of granitic crust by basaltic magma. Their closed-system thermal considerations yielded $r = 0{\cdot}34$ (Grove *et al.*, 1988, p. 339), whereas the geochemical data yielded $r = 1{\cdot}34$ for $F = 0{\cdot}68$ (Grove *et al.*, 1988, fig. 12). The former value ($r = 0{\cdot}34$, inverted triangle in Fig. 8b) is consistent with coupled heat and mass transfer in a crustal magma chamber. The latter value (line at $r = 1{\cdot}34$ in Fig. 8b) is not a possible solution for $F = 0{\cdot}68$, and could imply that fractionation and assimilation were not spatially or temporally concurrent. According to Grove *et al.* (1988, p. 320), the proportion of contaminated magmatic rock is less than the overall amount of erupted lava in their field area. Thus their data (Grove *et al.*, 1988, p. 320) could suggest that crystallization and assimilation were occurring at different places at different times.

REGIMES OF HIGHEST ASSIMILATION IN THE CONTINENTAL CRUST

For magmatic systems that include the crustal rocks adjacent to the magma body, heat transfer from a cooling mantle magma, which is fractionating and crystallizing (FC), must be able to travel fast enough to the crustal rocks for them to undergo partial melting in order for assimilation (A) to occur. Furthermore, the crustal melt must be able to segregate from its residue and undergo mass transfer for it to be able to mix with the mantle magma. Clearly, the optimal situation for assimilation is when the crustal rocks already contain partial melt, which then must segregate and migrate towards the high-temperature mantle magma.

Assimilation of melted crustal rocks by hydrous mantle magmas is most efficient (highest r values) for country rocks close to their melting point and for the most primitive (high-temperature) mantle magmas. Fractionally crystallizing hydrous picritic mantle magmas in their fractionation stage to olivine tholeiite (1350–1150°C) are able to ingest fairly cool (200°C) country rocks. For initial country rock temperatures >400°C, the amount of assimilation exceeds crystallization. Derivative magmatic liquids fractionating at <1200°C (e.g. basalt to basaltic andesite) can still assimilate fertile crustal rocks—those above 800°C with more assimilation than crystallization; those below 400°C with a constant, low degree of assimilation (Fig. 7).

Mixed magma compositions that have departed from the petrological liquid line of descent will return to this line through compensation by crystallization from the hybrid magma. This will leave signatures in the form of abundance of intermediate rock-types in fractionation series. By evaluating which aspects of AFC processes are thermally regulated and how this compares with F and r values deduced from certain geochemical signatures, we might be able to evaluate the variable dependence of FC upon A. This aspect is becoming increasingly important in trying to understand the significance of changes in magma composition and amount through time as an indication of the secular cooling of the Earth (e.g. Sparks, 1986), and as indicators for the chemical evolution of the continental crust (e.g. Rudnick, 1995; Rudnick *et al.*, 1998).

CONCLUSIONS

The results of our calculations include several aspects well known from other studies:

(1) the initial country rock temperature is the greatest limiting parameter for assimilation. The fertility with regard to melting potential of the crustal lithologies is an important parameter, but very fertile pelitic and quartzofeldspathic rocks at the base of continental crust (the ideal candidates for assimilation by mantle magmas) are only ~10% more efficiently assimilated than less fertile tonalite.

(2) Assimilation is enhanced for crustal rocks already at temperatures above the solidus of the country rock assimilate, mainly because the heat of fusion has already been supplied and also because the melt fraction in the assimilate increases with temperature.

(3) The potential for assimilation by a fractionating, hydrous, mantle-derived magma decreases from picritic to granodioritic compositions because of falling liquidus temperatures. Low country rock initial temperatures amplify this effect. Our main new conclusions may be summarized as follows:

(4) the thermal potential (total enthalpy) of a hydrous picritic parental magma offers the possibility for assimilation of an equal amount of crustal rocks at lower crustal depths through AFC processes, even for crustal temperatures appropriate to a standard geothermal gradient (e.g. at 30 km, $T = 600$°C for 20°C/km).

(5) The nature of the magma type (which can be obtained from mineral and bulk-rock compositions), and the related magma temperatures (which can be obtained from phase assemblages and geothermometry), can be used with our graphs to compare the extent of AFC processes based upon energy balance with the F and r values deduced from geochemical modelling.

(6) In general, to distinguish between compositional changes and volumes of the various calc-alkaline rock-types being due mostly to fractional crystallization (FC), or more to assimilation (A), is to determine in specific field areas at which stage in the histories contamination took place. Assimilation takes place most pronouncedly at higher temperature, i.e. during earlier magmatic stages. High-temperature cooling of hydrous picrite does not result in much early crystallization, and the heat released would promote crustal assimilation. This would increase the amount of intermediate members in calc-alkaline series in assimilation-dominated plutonic series, whereas in fractional crystallization dominated volcanic series the bimodal 'Daly Gap' is characteristic.

(7) In our models, AFC processes for hydrous basalt at high pressures result in much lower r values than realized for anhydrous MORB or HAB at lower pressures by Reiners *et al.* (1995). Thus at shallow crustal depths the high r value assimilation indicated for hot dry basaltic and andesitic intrusions will be able to affect only small rock volumes because of large sensible heat terms relative to low ambient crustal temperatures. Also, great variation in the degree of assimilation at a small scale [e.g. as reported by Grove *et al.* (1988)] will result.

(8) Because the presented thermal AFC calculations give maximum values (because we use a static heat balance rather than a full transport model) they thus provide realistic upper limits on the integrated amount of assimilation during the magmatic history. This can be used together with F and r values obtained from geochemical estimates to suggest the magma type and temperature of the assimilant, and hence constrain the geological evolution—the temperatures and hence depth of assimilation, the nature and geological location of the crustal assimilate, and the nature of the parent magma at the time of crystallization. This combined approach will be very useful to deduce the extent of crustal contamination in models of whole crustal evolution. Even within individual plutons our models may be used to examine the magnitudes of the various steps in AFC processes.

(9) In most cases of calc-alkaline intrusions, including the Adamello batholith, the amount of assimilation increases during gabbro to granite fractionation. Furthermore, assimilation occurs mainly where fertile crustal rocks are disaggregated into small xenoliths, and is favoured in lower crust preheated by the passage of previous magma.

ACKNOWLEDGEMENTS

This work was supported by ETH Research Credit 0-20-711-93. We thank Peter Nievergelt for drawing the figures, and Ursula Stidwill for checking the manuscript. We thank three anonymous reviewers and Steve Tait for very helpful comments, and George Bergantz and especially Marge Wilson for very considerate editing.

REFERENCES

Aitcheson, S. J. & Forrest, A. H. (1995). Quantification of crustal contamination in open magmatic systems. *Journal of Petrology* **35**, 461–488.

Anderson, A. T. (1980). Significance of hornblende in calc-alkaline andesites and basalts. *American Mineralogist* **65**, 837–851.

Barboza, S. A. & Bergantz, G. W. (1997). Melt productivity and rheology; complementary influences on the progress of melting. *Numerical Heat Transfer, Part A* **31**, 375–392.

Barth, A. P., Wooden, J. L., Tosdal, R. M. & Morrison, J. (1995). Crustal contamination in the petrogenesis of a calc-alkaline rock series: Josephine Mountain intrusion, California. *Geological Society of America Bulletin* **107**, 201–212.

Beard, J. S. & Lofgren, G. E. (1991). Dehydration melting and water-saturated melting of basaltic and andesitic greenstones and amphibolites. *Journal of Petrology* **32**, 365–401.

Bergantz, G. W. (1989). Underplating and partial melting: implications for melt generation and extraction. *Science* **245**, 1093–1095.

Bergantz, G. W. (1990). Melt fraction diagrams: the link between chemical and transport models. In: Nicholls, J. & Russell, J. K. (eds) *Modern Methods of Igneous Petrology. Mineralogical Society of America, Reviews in Mineralogy* **24**, 239–257.

Bergantz, G. W. & Dawes, R. (1994). Aspects of magma generation and ascent in continental lithosphere. In: Ryan, M. P. (ed.) *Magmatic Systems*. New York: Academic Press, pp. 291–317.

Berman, R. G. & Brown, T. H. (1985). Heat capacity of minerals in the system Na_2O–K_2O–CaO–MgO–FeO–Fe_2O_3–Al_2O_3–SiO_2–TiO_2–H_2O–CO_2: representation, estimation, and high-temperature extrapolation. *Contributions to Mineralogy and Petrology* **89**, 168–183.

Bigazzi, G., Del Moro, A. & Macera, P. (1986). A quantitative approach to trace element and Sr isotope evolution in the Adamello Batholith (Northern Italy). *Contributions to Mineralogy and Petrology* **94**, 46–53.

Blundy, J. D. & Shimizu, N. (1991). Trace element evidence for plagioclase recycling in calc-alkaline magmas. *Earth and Planetary Science Letters* **102**, 178–197.

Bohrson, W. A. & Spera, F. J. (2001). Energy-constrained open-system magmatic processes II: Application of energy-constrained assimilation and fractional crystallization (EC-AFC) model to magmatic systems. *Journal of Petrology* **42**, 1019–1041.

Bowen, N. L. (1922*a*). The reaction principle in petrogenesis. *Journal of Geology* **30**, 177–198.

Bowen, N. L. (1922*b*). The behaviour of inclusions in igneous magmas. *Journal of Geology* **30**, 513–570.

Callegari, E. (1983). Geological and petrological aspects of the magmatic activity at Adamello (northern Italy). *Memoire della Società Geologica Italiana* **26**, 83–103.

Callegari, E. & Dal Piaz, G. (1973). Field relationships between the main igneous masses of the Adamello massif (Northern Italy). *Memorie degli Istituto di Geologia e Mineralogia dell'Universita de Padova* **29**, 1–38.

Chappell, B. W. & White, A. J. R. (1974). Two contrasting granite types. *Pacific Geology* **8**, 173–174.

Cortecci, G., Del Moro, A., Leone, G. & Pardini, G. L. (1979). Correlation between strontium and oxygen isotopic compositions of rocks from the Adamello Massif (Northern Italy). *Contributions to Mineralogy and Petrology* **68**, 421–427.

Dal Piaz, G. V. & Venturelli, G. (1983). Brevi riflessioni sul magmatismo post-ofiolitico. *Memorie della Società Geologica Italiana* **26**, 5–19.

Davies, J. H. & Stevenson, D. J. (1992). Physical model of source region of subduction zone volcanics. *Journal of Geophysical Research* **97**, 2037–2070.

Del Moro, A., Ferrara, G., Tonarini, S. & Callegari, E. (1983*a*). Rb–Sr systematics on rocks from the Adamello batholith (Southern Alps). *Memorie della Società Geologica Italiana* **26**, 261–284.

Del Moro, A., Pardini, G. C., Quericioli, C., Villa, I. M. & Callegari, E. (1983*b*). Rb/Sr and K/Ar chronology of Adamello granitoids, Southern Alps. *Memorie della Società Geologica Italiana* **26**, 285–300.

DePaolo, D. J. (1981). Trace element and isotopic effects of combined wallrock assimilation and fractional crystallisation. *Earth and Planetary Science Letters* **53**, 189–202.

Dupuy, C., Dostal, J. & Fratta, M. (1982). Geochemistry of the Adamello Massif (Northern Italy). *Contributions to Mineralogy and Petrology* **80**, 41–48.

Gardien, V., Thompson, A. B., Grujic, D. & Ulmer, P. (1995). Melt fractions during crustal anatexis of biotite + plagioclase + quartz ± muscovite assemblages. *Journal of Geophysical Research* **100**, 15581–15591.

Ghiorso, M. S. (1985). Chemical mass transfer in magmatic processes I. Thermodynamic relations and numerical algorithms. *Contributions to Mineralogy and Petrology* **90**, 107–120.

Ghiorso, M. S. & Kelemen, P. B. (1987). Evaluating reaction stoichiometry in magmatic systems evolving under generalized thermodynamic constraints: examples comparing isothermal and isenthalpic assimilation. In: Mysen, B. O. (ed.) *Magmatic Processes: Physicochemical Principles. Geochemical Society of America, Special Publication* **1,** 319–336.

Gill, J. B. (1981). *Orogenic Andesites and Plate Tectonics*. Berlin: Springer, 390 pp.

Green, T. H. (1982). Anatexis of mafic crust and high pressure crystallization of andesite. In: Thorpe, R. S. (ed.) *Andesites: Orogenic Andesites and Related Rocks*. New York: Wiley, pp. 465–487.

Grove, T. L. & Baker, M. B. (1984). Phase equilibrium controls on the tholeiitic versus calc-alkaline differentition trends. *Journal of Geophysical Research* **89**, 3253–3274.

Grove, T. L., Kinzler, R. J., Baker, M. B., Donnelly-Nolan, J. M. & Lesher, C. E. (1988). Assimilation of granite by basaltic magma at Burnt Lava flow, Medicine Lake volcano, northern California: decoupling of heat and mass transfer. *Contributions to Mineralogy and Petrology* **99**, 320–343.

Hansmann, W. (1996). Age determinations of the Tertiary Madsino–Bregaglia (Bergell) intrusive (Italy, Switzerland): a review. *Schweizerische Mineralogische und Petrographische Mitteilungen* **76**, 421–451.

Hildreth, W. & Moorbath, S. (1988). Crustal contributions to arc magmatism in the Andes of Central Chile. *Contributions to Mineralogy and Petrology* **98**, 455–489.

Huppert, H. E. & Sparks, R. S. (1988). The generation of granitic magmas by intrusion of basalt into continental crust. *Journal of Petrology* **29**, 599–624.

Johnston, A. D. & Wyllie, P. J. (1988). Interaction of granitic and basic magmas: experimental observations on contamination processes at 10 kbar with H_2O. *Contributions to Mineralogy and Petrology* **98**, 352–362.

Kagami, H., Ulmer, P., Hansmann, W., Dietrich, V. & Steiger, R. H. (1991). Nd–Sr isotopic and geochemical characteristics of the southern Adamello (northern Italy) intrusives: implications for crustal versus mantle origin. *Journal of Geophysical Research* **96**, 14331–14346.

Kelemen, P. B. (1990). Reaction between ultramafic rock and fractionating basaltic magma I. Phase relations, the origin of calc-alkaline magmas series, and the formation of discordant dunite. *Journal of Petrology* **31**, 51–98.

Kelemen, P. B., Joyce, D. M., Webster, J. D. & Holloway, J. R. (1990). Reaction between ultramafic rock and fractionating basaltic magma II. Experimental investigation of reaction between olivine tholeiite and harzburgite at 1150–1050°C. *Journal of Petrology* **31**, 99–134.

Koyaguchi, T. (1990). Dynamics of mixing between mafic and silicic magmas: evidence from volcanic rocks. In: Marumo, F. (ed.) *Dynamic Processes of Material Transport and Transformation in the Earth's Interior*. Tokyo: Terra, pp. 357–376.

Koyaguchi, T. & Kaneko, K. (1999). A two-stage thermal evolution model of magmas in continental crust. *Journal of Petrology* **40**, 241–254.

Kress, V. C. & Carmichael, I. S. E. (1991). The compressibility of silicate liquids containing Fe_2O_3 and the effect of composition, temperature, oxygen fugacity and pressure on their redox states. *Contributions to Mineralogy and Petrology* **108**, 82–92.

Lange, R. L. & Carmichael, I. S. E. (1990). Thermodynamic properties of silicate liquids with emphasis on density, thermal expansion and compressibility. In: Nicholls, J. & Russell, J. K. (eds) *Modern Methods of Igneous Petrology. Mineralogical Society of America, Reviews in Mineralogy* **24**, 25–64.

Lange, R. L. & Navrotsky, A. (1992). Heat capacities of Fe_2O_3-bearing silicate liquids. *Contributions to Mineralogy and Petrology* **110**, 311–320.

Lange, R. L., De Yoreo, J. J. & Navrotsky, A. (1990). Scanning calorimetric measurement of heat capacity during incongruent melting of diopside. *American Mineralogist* **76**, 904–912.

Laubscher, H. P. (1983). The late Alpine (Periadriatic) intrusions and the Insubric Line. *Memoire della Società Geologica Italiana* **26**, 21–30.

Lesher, C. E. (1990). Decoupling of chemical and isotopic exchange during magma mixing. *Nature* **344**, 235–237.

Macera, P., Ferrara, G., Pescia, A. & Callegari, E. (1983). A geochemical study on the acid and basic rocks of the Adamello batholith (Southern Alps). *Memorie della Società Geologica Italiana* **26**, 223–259.

Mantovani, M. S. M. & Hawkesworth, C. J. (1990). An inversion approach to assimilation and fractional crystallisation processes. *Contributions to Mineralogy and Petrology* **105**, 289–302.

Marsh, B. D. & Maxey, M. R. (1985). On the distribution and separation of crystals in convecting magma. *Journal of Volcanology and Geothermal Research* **24**, 95–150.

Matile, L. (1996). Aufstieg und Platznahme von kalk-alkalinen Magmen—der Adamello-Batholith als Beispiel. PhD Dissertation, ETH-Zürich, 269 pp.

Matile, L., Thompson, A. B. & Ulmer, P. (2000). A fractionation model for hydrous calc-alkaline plutons and the heat budget during fractional crystallization and assimilation. In: Bagdassarov, N., Laporte, D. & Thompson, A. B. (eds) *Lectures on the Physics of Partially Molten Rocks*. Dordrecht: Kluwer Academic, pp. 179–208.

McLeod, P. & Sparks, R. S. J. (1998). The dynamics of xenolith assimilation. *Contributions to Mineralogy and Petrology* **132**, 21–33.

Navrotsky, A., Zeigler, D., Oestrike, R. & Manier, P. (1989). Calorimetry of silicate melts at 1773 K: measurement of enthalpies of fusion and of mixing in the system diopside–anorthite–albite and anorthite–forsterite. *Contributions to Mineralogy and Petrology* **101**, 122–130.

Nicholls, J. & Stout, M. Z. (1982). Heat effects of assimilation, crystallisation, and vesiculation in magmas. *Contributions to Mineralogy and Petrology* **81**, 328–339.

Nimis, P. & Ulmer, P. (1998). Clinopyroxene geobarometry of basic magmas: an expanded structural geobarometer for anhydrous and hydrous system. *Contributions to Mineralogy and Petrology* **133**, 122–135.

Pankhurst, R. J., Hole, M. J. & Brook, M. (1988). Isotope evidence for the origin of Andean granites. *Transactions of the Royal Society of Edinburgh, Earth Sciences* **79**, 123–133.

Patchett, P. J. (1980). Thermal effects of basalt on continental crust and crustal contamination of magmas. *Nature* **283**, 559–561.

Patiño Douce, A. E. & Beard, J. S. (1995). Dehydration melting of biotite gneiss and quartz amphibolite from 3 to 15 kbar. *Journal of Petrology* **36**, 707–738.

Raia, F. & Spera, F. J. (1997). Simulations of crustal anatexis: implications for the growth and differentiation of continental crust. *Journal of Geophysical Research* **102**, 22629–22648.

Reiners, P. W., Nelson, B. K. & Ghiorso, M. S. (1995). Assimilation of felsic crust and its partial melt by basaltic magma: thermal limits and extents of crustal contamination. *Geology* **23**, 563–566.

Reiners, P. W., Nelson, B. K. & Nelson, S. W. (1996). Evidence for multiple mechanisms of crustal contamination of magma from compositionally zoned plutons and associated ultramafic intrusions of the Alaska Range. *Journal of Petrology* **36**, 261–292.

Reusser, E. (1987). Phasenbeziehungen im Tonalit der Bergeller Intrusion. *Schweizerische Mineralogische und Petrographische Mitteilungen* **67**, 377–378.

Richet, P. & Bottinga, Y. (1986). Thermochemical properties of silicate glasses and liquids: a review. *Reviews of Geophysics* **24**, 1–25.

Ricklin, K. (1985). Contact metamorphism of the Permian 'Red Sandstones' in the Adamello Area. *Memorie della Società Geologica Italiana* **26**, 159–169.

Roberts, M. P. & Clemens, J. D. (1995). Feasibility of AFC models for the petrogenesis of calc-alkaline magma series. *Contributions to Mineralogy and Petrology* **121**, 139–147.

Romer, R. L., Schaerer, U. & Steck, A. (1996). Alpine and pre-Alpine magmatism in the root zone of the western Alps. *Contributions to Mineralogy and Petrology* **123**, 138–158.

Rudnick, R. L. (1995). Making continental crust. *Nature* **378**, 571–578.

Rudnick, R. L., McDonough, W. F. & O'Connell, R. J. (1998). Thermal structure, thickness and composition of continental lithosphere. *Chemical Geology, Special Issue: Geochemical Earth Reference Model* **145**, 399–416.

Russell, J. K. (1990). Magma mixing processes: insights and constraints from thermodynamic calculations. In: Nicholls, J. & Russell, J. K. (eds) *Modern Methods of Igneous Petrology. Mineralogical Society of America, Reviews in Mineralogy* **24**, 153–190.

Rutter, M. J. & Wyllie, P. J. (1988). Melting of vapor-absent tonalite at 10 kbar to simulate dehydration melting in the deep crust. *Nature* **331**, 159–160.

Sisson, T. W. & Grove, T. L. (1993). Experimental investigations of the role of H_2O in calc-alkaline differentiation and subduction zone magmatism. *Contributions to Mineralogy and Petrology* **113**, 143–166.

Sobolev, A. V. & Chaussidon, M. (1996). H_2O concentration in primary melts from supra-subduction zones and mid-ocean ridges: implications for H_2O storage and recycling in the mantle. *Earth and Planetary Science Letters* **137**, 45–55.

Sparks, R. S. J. (1986). The role of crustal contamination in magma evolution through geological time. *Earth and Planetary Science Letters* **78**, 211–223.

Sparks, R. S. J. & Marshall, A. L. (1986). Thermal and mechanical constraints on mixing between mafic and silicic magmas. *Journal of Volcanology and Geothermal Research* **29**, 99–124.

Spera, F. J. & Bohrson, W. A. (2001). Energy-constrained open-system magmatic processes I: General model and energy-constrained assimilation and fractional crystallization (EC-AFC) formulation. *Journal of Petrology* **42**, 999–1018.

Taylor, H. P., Jr (1980). The effects of assimilation of country rocks by magmas on $^{18}O/^{16}O$ and $^{87}Sr/^{86}Sr$ systematics in igneous rocks. *Earth and Planetary Science Letters* **47**, 243–254.

Thompson, A. B. (1996). Fertility of crustal rocks during anatexis. *Transactions of Royal Society of Edinburgh, Earth Sciences* **87**, 1–10.

Thompson, R. N., Dickin, A. P., Gibson, I. L. & Morrison, M. A. (1982). Elemental fingerprints of isotopic contamination of Hebridean Palaeocene mantle derived magmas and implications for mafic enclaves. *Contributions to Mineralogy and Petrology* **79**, 159–168.

Trümpy, R. (1973). The timing of orogenic events in the Central Alps. In: de Jong, K. A. & Scholten, R. (eds) *Gravity and Tectonics*. New York: Wiley pp. 229–251.

Trümpy, R. (1975). Penninic–Austroalpine boundary in the Swiss Alps: a presumed former continental margin and its problems. *American Journal of Science* **275-A**, 209–238.

Ulmer, P. (1982). Monticellite–clintonite bearing assemblages at the Southern border of the Adamello Massif. *Rendiconti della Società Italiana di Mineralogia e Petrografia* **38**, 617–628.

Ulmer, P. (1986). Basische und ultrabasische Gesteine des Adamello (Provinzen Brescia und Trento, Norditalien). Ph.D. Dissertation, ETH-Zürich.

Ulmer, P. (1989). High pressure phase equilibria of a calc-alkaline picro-basalt: implications for the genesis of calc-alkaline magmas. *Annual Report, Director of the Geophysical Laboratory, Carnegie Institution of Washington* **88**, 28–35.

Ulmer, P., Callegari, E. & Sonderegger, U. C. (1983). Genesis of the mafic and ultramafic rocks and their genetical relations to the tonalitic–trondhjemitic granitoids of the southern part of the Adamello batholith (northern Italy). *Memorie della Società Geologica Italiana* **26**, 171–222.

Vielzeuf, D. & Holloway, J. R. (1988). Experimental determination of the fluid-absent melting relations in the pelitic system. *Contributions to Mineralogy and Petrology* **98**, 257–276.

von Blanckenburg, F., Früh-Green, G., Diethelm, K. & Stille, P. (1992). Nd-, Sr-, O-isotopic and chemical evidence for a two-stage contamination history of mantle magma in the Central-Alpine Bergell intrusion. *Contributions to Mineralogy and Petrology* **110**, 33–45.

von Blanckenburg, F., Kagami, H., Deutsch, H., Oberli, F., Meier, M., Wiedenbeck, M., Barth, S. & Fischer, H. (1998). The origin of Alpine plutons along the Periadriatic lineament. *Schweizerische Mineralogische und Petrographische Mitteilungen* **78**, 55–66.

Watson, B. E. (1982). Basalt contamination by continental crust: some experiments and models. *Contributions to Mineralogy and Petrology* **80**, 73–87.

Werling, E. (1992). Tonale-, Pejo- und Judicarien Linie: Mikrostruktren und Metamorphose von tektoniten aus raeumlichen interferierenden aber verschiedenaltrige Verwerfungszonen. Dr. nat. Sci. Dissertation, ETH Zürich, 303 pp.

Wright, T. L. & Doherty, P. C. (1977). A linear programming and least squares computer method for solving petrologic mixing problems. *Geological Society of America Bulletin* **81**, 1995–2008.

Wyllie, P. J. (1977). Crustal anatexis: an experimental review. *Tectonophysics* **43**, 41–71.